

# Application of Laser Pulse Photoinjection of Electrons from Metal Electrodes to the Determination of Reduction Potentials of Organic Radicals in Aprotic Solvents

Philippe Hapiot, Valery V. Konovalov,<sup>1</sup> and Jean-Michel Savéant\*

Contribution from the Laboratoire d'Electrochimie Moléculaire de l'Université Denis Diderot (Paris 7), Unité de Recherche Associée au CNRS N° 438, 2 place Jussieu, 75251 Paris Cedex 05, France

Received October 13, 1994<sup>®</sup>

**Abstract:** Photoinjection of electrons from metal electrodes by means of a laser pulse can be used to interrogate the reduction of radicals in aprotic solvents such as DMF, DMSO, and acetonitrile. Since the generating substrates must be more difficult to reduce than the resulting radicals, the method appears as complementary to the direct electrochemical method. The procedure that allows the extraction of the radical current-potential curve from the transient coulometric photopotential is illustrated with the reduction of several arylmethyl radicals. The reduction potentials thus obtained are compared with previous determinations by other methods.

Reduction and oxidation potentials of organic radicals are often an important piece of knowledge for the comprehension of reactions mechanisms. Associated with similar information concerning the substrate from which the radical originates, it allows one to predict whether homogeneous or heterogeneous (electrodes) outersphere electron donors may trigger a radical chemistry or an ionic chemistry.<sup>2</sup> When a precise thermodynamical meaning can be assigned to such reduction or oxidation potentials, they may be used in appropriate cycles to derive other thermodynamical quantities such as bond energies and  $pK_a$ 's.<sup>3</sup>

One approach to the reduction potential of radicals is the electrochemical determination of the oxidation potential of the parent carbanion.<sup>4</sup> However, the values thus obtained must be carefully corrected from the decay kinetics of the ensuing radical.<sup>4a</sup> In the case of carbon-centered system, the carbanion is introduced as an organometallic derivative.<sup>4b</sup> In most cases, the influence of the metal cation on the kinetics and thermodynamics of the oxidation reaction is then difficult to unravel.

Direct application of electrochemical techniques, such as cyclic voltammetry, is possible when the parent substrate is easier to reduce (or to oxidize) than the radical under examination. This method has been used for a few carbon-centered radicals in acetonitrile.<sup>5ab</sup> It should be noted that the reduction potentials thus obtained contain kinetic factors pertaining to the decay of the radical and of the ensuing carbanion and to the electron transfer reaction. These factors should be taken into

account in the extraction of the standard potential from raw data.<sup>5</sup>

An indirect electrochemical approach, using redox catalysis,<sup>6</sup> has also been used for determining reduction potentials of alkyl radicals ( $R^\bullet$ ) in *N,N'*-dimethylformamide.<sup>7</sup> The substrate, usually an alkyl halide, gives rise to the corresponding radical by dissociative electron transfer from an electrochemically generated aromatic anion radical in a cyclic voltammetric experiment. The alkyl radical thus produced undergoes two competitive reactions with the aromatic anion radical, namely electron transfer reduction and coupling. The first of these reactions regenerates the aromatic hydrocarbon from which the aromatic anion radical derives thus giving rise to a redox catalytic current.<sup>6</sup> The second is the last step of a two-electron reduction. The rate ratio of the two competitive reactions can thus be derived from the normalized height of the cyclic voltammetric peak of the aromatic hydrocarbon in the presence of the alkyl halide.<sup>7,8</sup> Given the alkyl radical, the rate constant of the second reaction does not vary much with the nature of the aromatic anion radical. The rate of the first reaction increases as the standard potential of the aromatic hydrocarbon/aromatic anion radical couple becomes more and more negative. Assuming that the coupling rate constant is independent of the aromatic anion radical, an activation-driving force plot of the electron transfer to the alkyl radical may thus be derived from experiments in which the aromatic anion radical has been systematically varied. It is then possible to use the Marcus–Hush theory to estimate the formal potential and the intrinsic barrier of the  $R^\bullet/R^-$  couple albeit with a large uncertainty that is difficult to predict as in the direct electrochemical case.

A photoelectrochemical method in which the radical is

<sup>®</sup> Abstract published in *Advance ACS Abstracts*, January 1, 1995.

(1) Present address: Institute of Chemical Kinetics and Combustion SB RAS, 630090 Novosibirsk, Russia.

(2) (a) Savéant, J.-M. *Adv. Phys. Org. Chem.* **1990**, *26*, 1. (b) Savéant, J.-M. *Acc. Chem. Res.* **1993**, *26*, 455. (c) Savéant, J.-M. *Tetrahedron (Report No. 360)* **1994**, *50*, 10117.

(3) (a) Bordwell, F. G.; Cheng, J.-P.; Harrelson, J. A. *J. Am. Chem. Soc.* **1988**, *110*, 1229. (b) Bordwell, F. G.; Zhang, X.-M. *Acc. Chem. Res.* **1993**, *26*, 510. (c) Wayner, D. D. M.; Parker, V. D. *Acc. Chem. Res.* **1993**, *26*, 4287.

(4) (a) Andrieux, C. P.; Hapiot, P.; Pinson, J.; Savéant, J.-M. *J. Am. Chem. Soc.* **1993**, *115*, 7783. (b) Jaun, B.; Schwartz, J.; Breslow, R. *J. Am. Chem. Soc.* **1980**, *102*, 5741.

(5) (a) Andrieux, C. P.; Gallardo, I.; Savéant, J.-M. *J. Am. Chem. Soc.* **1989**, *111*, 1620. (b) Andrieux, C. P.; Grzeszczuk, M.; Savéant, J.-M. *J. Am. Chem. Soc.* **1991**, *113*, 8811. (c) Andrieux, C. P.; Grzeszczuk, M.; Savéant, J.-M. *J. Electroanal. Chem.* **1991**, *318*, 369.

(6) (a) Andrieux, C. P.; Savéant, J.-M. *Electrochemical Reactions. In Investigation of Rates and Mechanisms of Reactions, Techniques of Chemistry*; Bernasconi, C. F., Ed.; Wiley: New York, 1986; Vol. VI/4E, Part 2, pp 305–390. (b) Andrieux, C. P.; Hapiot, P.; Savéant, J.-M. *Chem. Rev.* **1990**, *90*, 723.

(7) (a) Fuhendorff, R.; Occhialini, D.; Pedersen, S. U.; Lund, H. *Acta Chem. Scand.* **1989**, *43*, 803. (b) Occhialini, D.; Daasbjerg K.; Lund, H. *Acta Chem. Scand.* **1990**, *44*, 711. (c) Occhialini, D.; Pedersen, S. U.; Lund, H. *Acta Chem. Scand.* **1990**, *44*, 715. (c) Occhialini, D.; Kristensen, J. S.; Daasbjerg K.; Lund, H. *Acta Chem. Scand.* **1992**, *46*, 474. (c) Occhialini, D.; Daasbjerg K.; Lund, H. *Acta Chem. Scand.* **1993**, *47*, 1100.

(8) Nadjó, L.; Savéant, J.-M.; Su, K. B. *J. Electroanal. Chem.* **1985**, *196*, 23.

generated by photolysis of a substrate with modulated light and the in-phase current-potential curve for its reduction or oxidation at a grid electrode is recorded has been extensively used for determining reduction and oxidation potentials of radicals in acetonitrile.<sup>9</sup> The difference between these reduction or reduction potentials and the corresponding formal potentials due to kinetic factors is difficult to estimate with the grid working electrode that was used in these studies. A more precise estimation of the kinetic factor has been made in the case of the diphenylmethyl radical where a small microdisk electrode was used.<sup>10</sup>

Polarograms of radicals generated from organic substrates by pulse radiolysis in water have also been reported.<sup>11</sup>

A different photoelectrochemical approach to the reduction potentials of radicals may be followed. It consists in injecting electrons from a metal electrode by means of a laser pulse or of modulated light and in observing their reaction with a substrate introduced in the solution. The irradiation wavelength is selected in a range where the absorption of the substrate is weak. The fundamentals of such photoinjection of electrons have been described in the late 1960s.<sup>12ab</sup> Follow-up studies (dependence of photocurrent on electron scavenger concentration, wavelength, polarization and angle of incident light, nature of metal and electrode double layer) have demonstrated the existence of photoinjection from the metal to the solution and its similarities with photoemission from metals into vacuum.<sup>12</sup> The method has been applied to the determination of thermalization lengths of slow electrons in polar liquids<sup>12f,13</sup> as well as to detection of short-lived intermediates resulting from the capture of solvated electrons thus generated and estimation of the rate constants of bulk and electrode reactions they may undergo.<sup>14,15</sup> Measuring the photogenerated charge as a function of the dc potential applied to the working electrode one may obtain current-potential curves (photopolarograms) character-

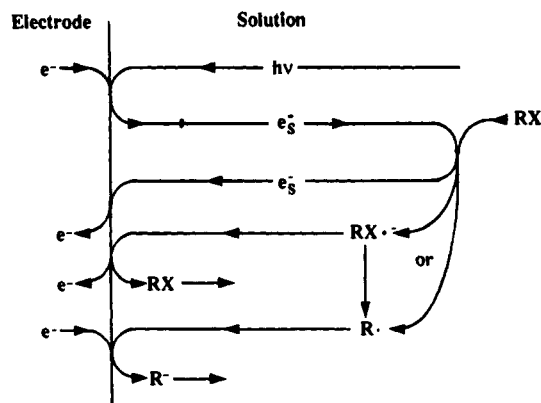


**Figure 1.** Photoinjection of electrons from the electrode and ensuing reactions.

izing the reduction of transient electron capture intermediates. For example, photopolarograms at a mercury electrode have been recorded in aqueous solution for the following species: H-atom,<sup>14a,d,g</sup> simple alkyl radicals (CH<sub>3</sub>, C<sub>2</sub>H<sub>5</sub>),<sup>12d,14c,h</sup> hydroxyalkyl radicals (CH<sub>2</sub>OH),<sup>14a,h</sup> and inorganic anion radicals (NO<sub>3</sub><sup>2-</sup>, NO<sub>2</sub><sup>2-</sup>,<sup>14a,b</sup> BrO<sub>2</sub>,<sup>14a</sup> CO<sub>2</sub><sup>-</sup>,<sup>14e,g</sup>) and, more recently, for several substituted phenyl radicals.<sup>15</sup>

Much less attention has been paid to photoinjection of electrons into aprotic solvents such as the classical solvents of organic electrochemistry (*N,N'*-dimethylformamide (DMF), dimethyl sulfoxide (DMSO), acetonitrile) and from electrode metals other than mercury. In this respect, investigations have been restricted to the observation of photocurrents upon illumination of various metals (Hg, Au, Ag) and estimation of the corresponding threshold potentials.<sup>16</sup> So far, photoinjection of electrons has not been used to investigate the reduction of transient intermediates in such solvents. This is an important objective in view of the uncertainties embodied in the various methods that have been used so far as discussed earlier. Comparison between results obtained by independent methods will help to understand the exact meaning of the reduction potentials that are measured in each case. The work described below aimed at demonstrating the applicability of the electron photoinjection method to the determination of reduction potentials of transient intermediates in aprotic solvents. Since benzyl, substituted benzyl, and diphenylmethyl radicals have been widely investigated by the other methods, we focused attention on these radicals for comparison purposes.

## Results and Discussion

The principle of the method is summarized in Figure 1. Upon illumination of the electrode, electrons are transferred to the solution. After fast thermalization and solvation ( $t_s \approx 10^{-13}$ – $10^{-12}$  s), the solvated electrons ( $e_s^-$ ) thus produced decay over a distance from the electrode  $l_s = 10$ – $60$  Å ( $10$ – $60$  Å in water,<sup>13</sup>  $10$ – $20$  Å, in methanol<sup>16e</sup>). At longer times, solvated electrons competitively diffuse back to the electrode ( $t_d = l_s^2/D_e \approx 10^{-9}$  s) where they are instantaneously reoxidized or react in the solution with the solvent or with a purposely added scavenger, RX, from which the radical R<sup>•</sup> will be produced.

If all solvated electrons diffuse back to the electrode surface, the net photoinjected charge is zero. RX is therefore selected so as to be rapidly reduced by solvated electrons. Since solvated electrons are potent reducing agents (standard potential in

(9) (a) Sim, B. A.; Griller, D.; Wayner, D. D. M. *J. Am. Chem. Soc.* **1989**, *111*, 754. (b) Griller, D.; Simões, J. A. M.; Mulder, P.; Wayner, D. D. M. *J. Am. Chem. Soc.* **1989**, *111*, 7872. (c) Nagaoka, T.; Berinstain, A. B.; Griller, D.; Wayner, D. D. M. *J. Org. Chem.* **1990**, *55*, 3707. (d) Sim, B. A.; Milne, P. H.; Griller, D.; Wayner, D. D. M. *J. Am. Chem. Soc.* **1990**, *112*, 6635.

(10) Smith, D. K.; Strohhben, W. E.; Evans, D. H. *J. Electroanal. Chem.* **1990**, *288*, 111.

(11) Henglein, A. *Electroanalytical Chemistry*, Bard, A. J., Ed.; Dekker: New York, 1976; Vol. 9, pp 163–244.

(12) (a) Barker, G. C.; Gardner, A. W.; Sammon, D. C. *J. Electrochem. Soc.* **1966**, *113*, 1182. (b) Barker, G. C. *Ber. Bunsenges. Phys. Chem.* **1971**, *75*, 728. (c) Pleskov, Y. V.; Rotenberg, Z. A. *J. Electroanal. Chem.* **1969**, *20*, 1. (d) Gurevich, Y. Y.; Pleskov, Y. V.; Rotenberg, Z. A. *Photoelectrochemistry*; Plenum Press: New York, 1980. (e) Benderskii, V. A.; Babenko, S. D.; Krivenko, A. G.; Zolotovskii, Y. M.; Rudenko, T. S. *J. Electroanal. Chem.* **1974**, *56*, 325. (f) Babenko, S. D.; Benderskii, V. A.; Zolotovskii, Y. M.; Krivenko, A. G.; *J. Electroanal. Chem.* **1977**, *76*, 347. (g) Benderskii, V. A.; Brodsky, A. M. *Photoemission from Metals into Electrolyte Solutions*; Nauka, Moscow, 1977 (in Russian). (h) Konovalov, V. V.; Raitsimring, A. M.; Tsvetkov, Y. D. *J. Electroanal. Chem.* **1990**, *292*, 33.

(13) Konovalov, V. V.; Raitsimring, A. M.; Tsvetkov, Y. D. *Radiat. Phys. Chem.* **1988**, *32*, 623.

(14) (a) Barker, G. C.; McKeown, D.; Williams, M. J.; Bottura, G.; Concialini, V. *Discuss. Faraday. Soc.* **1974**, *56*, 41. (b) Pleskov, Y. V.; Rotenberg, Z. A.; Eletsky, V. V.; Lakomov, V. I. *Discuss. Faraday. Soc.* **1974**, *56*, 52. (c) Schiffrin, D. *Discuss. Faraday. Soc.* **1974**, *56*, 75. (d) Ovchinnikov, A. A.; Benderskii, V. A.; Babenko, S. D.; Krivenko, A. G. *J. Electroanal. Chem.* **1978**, *91*, 321. (e) Babenko, S. D.; Benderskii, V. A.; Krivenko, A. G.; Kurmaz, V. A. *J. Electroanal. Chem.* **1983**, *159*, 163. (f) Rotenberg, Z. A.; Ruffman, N. M. *J. Electroanal. Chem.* **1984**, *175*, 153. (g) Benderskii, V. A.; Krivenko, A. G.; Fedorovich, N. V. *J. Electroanal. Chem.* **1988**, *241*, 247. (h) Benderskii, V. A.; Krivenko, A. G. *Usp. Khim.* **1990**, *59*, 3 (Engl transl: *Russian Chem. Rev.* **1990**, *59*, 1.). (i) Kalugin, A. I.; Konovalov, V. V.; Raitsimring, A. M. *J. Electroanal. Chem.* **1993**, *362*, 185.

(15) (a) Konovalov, V. V.; Raitsimring, A. M.; Tsvetkov, Y. D.; Bilkis, I. I. *Chem. Phys. Lett.* **1989**, *157*, 257. (b) Konovalov, V. V.; Tsvetkov, Y. D.; Bilkis, I. I.; Laev, S. S.; Shteingarts, V. D. *Mendeleev Commun.* **1993**, *39*. (c) Konovalov, V. V.; Bilkis, I. I.; Selinavov, B. A.; Shteingarts, V. D.; Tsvetkov, Y. D. *J. Chem. Soc., Perkin Trans. 2* **1993**, 1707.

(16) (a) Yamashita, K.; Himai, I. *Electrochimica Acta* **1977**, *18*, 1697. (b) Kokilashvili, R. G.; Yeletsii, V. V.; Pleskov, Yu. V. *Electrochimica Acta* **1984**, *29*, 1075. (c) Itaya, K.; Malpas, R. E.; Bard, A. J. *J. Chem. Phys. Lett.* **1979**, *63*, 411. (d) Harima, Yu.; Sato, H.; Suga, K. *J. Phys. Chem.* **1989**, *93*, 6418. (e) Kalugin, A. I.; Konovalov, V. V.; Raitsimring, A. M. *J. Electroanal. Chem.* **1993**, *359*, 63.

water:  $-3.1$  V vs SCE<sup>17</sup>), this condition leaves open a large range of choice for radical generating scavengers with a rate constant of electron attachment,  $k_e$ , close to the diffusion limit ( $\approx 10^{10} \text{ M}^{-1} \text{ s}^{-1}$ ). Under these conditions, scavenger concentrations ( $C^0$ ) of the order of 10–100 mM are sufficient for trapping a significant portion of the solvated electrons. If the anion radical,  $\text{RX}^{\bullet-}$ , resulting from electron attachment is chemically stable, it diffuses back to the electrode where it is instantaneously reoxidized; and the net photoinjected charge is again zero. However, if  $\text{RX}^{\bullet-}$  rapidly decomposes into  $\text{R}^{\bullet}$  and  $\text{X}^-$ , or if  $\text{RX}$  undergoes a dissociative electron attachment, there is a net photoinjected charge corresponding to the generation of electrochemically stable  $\text{X}^-$  ions. A thin layer of  $\text{R}^{\bullet}$  radicals, adjacent to the electrode surface is thus produced.

During each experiment, the dc electrode potential is maintained at a fixed value that can be changed from one experiment to the other. If the dc potential is more positive than the reduction potential of  $\text{R}^{\bullet}$  (and more negative than its oxidation potential), the net photoinjected charge is a reflection of the stoichiometry of electron attachment to the scavenger (1 in the applications developed below). Conversely, if the dc potential is more negative than the reduction potential of  $\text{R}^{\bullet}$ , the net photoinjected charge corresponds to the electron required for generating  $\text{R}^{\bullet}$  plus the electron required to reduce  $\text{R}^{\bullet}$  into  $\text{R}^-$ . Thus upon varying the dc potential between these two limits, the net photoinjected charge is expected to reflect the variation of the electron stoichiometry for the reduction of  $\text{R}^{\bullet}$ ,  $n(E)$ . In other words, determination of the net photoinjected charge as a function of the dc potential should lead to a "polarogram" which half-wave potential would be a measure of the reduction potential of  $\text{R}^{\bullet}$ .

It appears from the representation of the electrical equivalent circuit of the cell and of the experimental setup given in Figure 2 that what is actually measured is the photopotential  $\Delta E_{\text{ph}}(t)$  that is related to the photoinjected charge  $Q(t)$  according to eq 1

$$\Delta E_{\text{ph}}(t) = \frac{R_s}{(R_s + R_c)C_d} \int_0^t i_{\text{ph}}(\tau) \exp\left[-\frac{t-\tau}{(R_s + R_c)C_d}\right] d\tau \approx \frac{R_s}{(R_s + R_c)C_d} Q(t) \exp\left[-\frac{t}{(R_s + R_c)C_d}\right] \quad (1)$$

( $i_{\text{ph}}$ , photocurrent;  $R_c$ , cell resistance;  $R_s$ , sampling resistance;  $C_d$ , double layer capacitance).

The applicability of eq 1 is illustrated in Figure 3 in the case of benzyl bromide in DMF at a gold electrode for several values of the sampling resistance. It follows that with sufficiently large values of the sampling resistance, i.e., large RC times, and for observation times of the order of 200  $\mu\text{s}$  as used in the following experiments:

$$\Delta E_{\text{ph}}(t) \approx \frac{Q(t)}{C_d} \quad (2)$$

Under such conditions, the photoinjected charge is coulombically stored in the double layer capacitance. The achievement of such a situation where leaking of charge from the double layer capacitance can be neglected also requires that the faradaic impedance shown in Figure 2 be large, i.e., that the direct reduction of  $\text{RX}$  at the electrode is insignificant in the potential range where the photoinjection experiments are performed. We accordingly observed that the photopotential decreases rapidly when the dc potential reaches values where the cyclic voltammetric wave of the scavenger develops. Application of the

(17) Hart, E. J.; Anbar, M. *Hydrated Electron*; Wiley: New York, 1970.

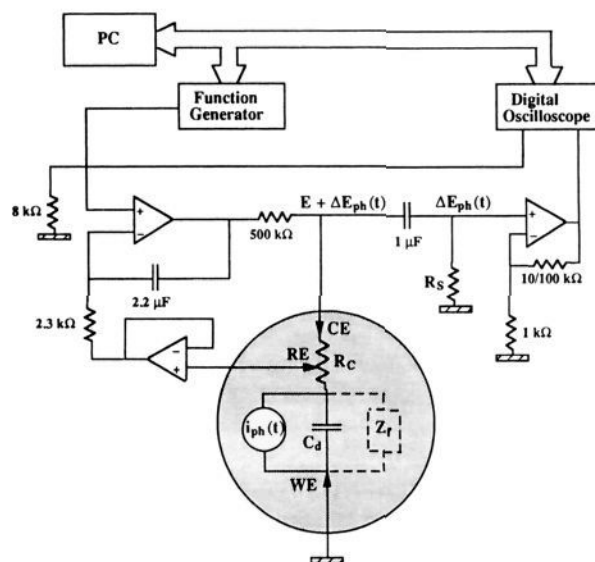


**Figure 2.** Equivalent circuit of the cell and experimental setup:  $E$ , dc potential;  $\Delta E_{\text{ph}}(t)$ , photopotential;  $i_{\text{ph}}$ , photocurrent;  $R_c$ , cell resistance;  $R_s$ , sampling resistance;  $C_d$ , double layer capacitance;  $Z_f$ , faradaic impedance.

photoinjection technique to the determination of reduction potentials of radical is thus complementary to the direct electrochemical method which conversely requires that the radical is more difficult to reduce than  $\text{RX}$ .

As seen in Figure 3, the photopotential is very small, on the order of a few millivolts. It follows that it can be neglected when the dependence of the photoinjected charge,  $Q$ , and hence of the electron stoichiometry,  $n(E)$ , upon electrode potential is sought.

The photoinjected charge is related to the radical reduction electron stoichiometry,  $n(E)$ , and to various other factors through equation (3).<sup>12g,16c</sup>

$$Q(E)/Q_0 = [1 + n(E)] \left[ 1 - \int_0^\infty \exp(-x/l_e) f(x) dx \right] = [1 + n(E)] F(E, C^0) \quad (3)$$

$Q_0$  is the photoinjected total charge,  $x$  the distance from the electrode surface,  $f(x)$  the initial spatial distribution of solvated electrons,  $l_e = (D_e/k_e C^0)^{1/2}$  the reaction-diffusion layer thickness for electron attachment.  $Q_0$  depends on the electrode potential according to the 5/2 power law expressed in eq 4.<sup>18</sup>

$$Q_0(E) = A(E - E_{\text{thr}})^{5/2} \quad (4)$$

where  $E_{\text{thr}}$  is the threshold potential for photoinjection and  $A$  is a coefficient proportional to the photon flux. Equation 5 ensues.

$$Q(E) = A(E - E_{\text{thr}})^{5/2} F(E, C^0) [1 + n(E)] \quad (5)$$

Figure 4 gives a first test of eq 5 for a substrate, 4-bromoanisole, that generates a radical, 4-methoxyphenyl, which is completely reduced in the whole range of investigated potentials.<sup>19</sup> Both in acetonitrile with a mercury electrode and in DMF with a gold electrode, plots of  $Q(E)^{2/5}$  vs potential in the presence and absence of the scavenger are linear and intersect the potential axis at the same potential. This observation indicates that the 5/2 power law is satisfactorily followed and that the function  $F(E, C^0)$  is practically independent of potential.

(18) Brodsky, A. M.; Gurevich, Y. Y. *Zh. Eksp. Teor. Fiz.* **1968**, *54*, 213.

(19) (a) Aryl radicals have reduction potentials around 0.3–0.5 V vs SCE.<sup>4b,19b</sup> (b) Savéant, J.-M. *J. Phys. Chem.* **1994**, *94*, 3716.

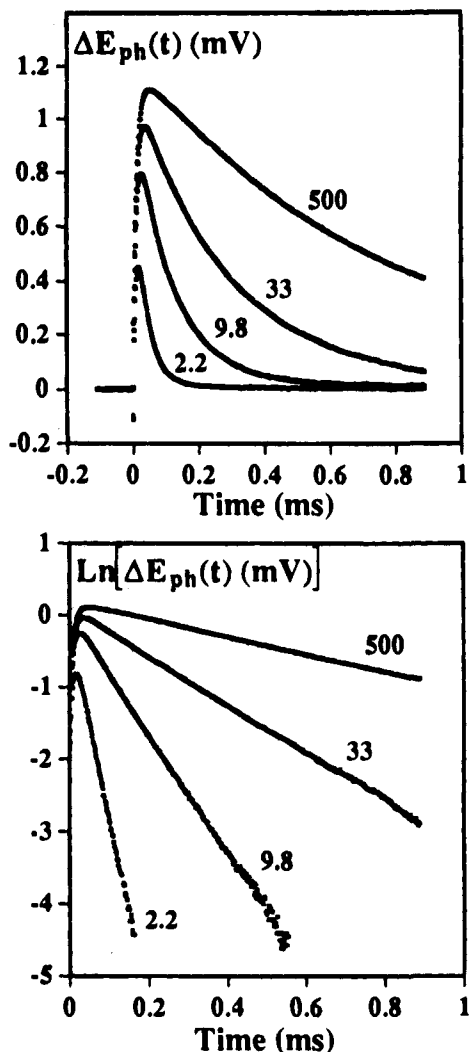


**Figure 3.** Time dependence of the photopotential,  $\Delta E_{ph}(t)$ , for the reduction of 10 mM benzyl bromide in DMF (+0.1 M  $\text{Et}_4\text{NClO}_4$ ) at a gold disk electrode. Dc potential:  $-1.45$  V vs SCE. The number on each curve is the value of the sampling resistance in  $\text{k}\Omega$ .

The intersection of the linear plot with the potential axis then provides the values of the threshold potential (Table 1). The same conclusion applies to scavengers generating benzylic radicals as illustrated by the reduction of 4-methylbenzyl chloride in DMSO, DMF, and acetonitrile (Figure 5).

In this case, the polarogram of the radical is visible in the range of potential investigated. The straight lines that appear at the low and high potential limits respectively intersect the potential axis at the same (threshold) potential. The values of the threshold potentials thus estimated are summarized in Table 1.

Figure 6 illustrates the procedure that can be used to extract the polarogram of a radical from the raw data. The  $Q(E)^{2/5}$  straight line obtained at the foot of the reduction wave is used as the denominator of the ratio from which  $1 + n(E)$  is derived according to equation 6.

$$[1 + n(E)] = \frac{Q(E)}{A(E - E_{thr})^{5/2} F(E, C^0)} \quad (6)$$

Although not central to the derivation of the radical polarogram from the raw data, it is interesting to investigate the effect of the scavenger concentration on the photoresponses as predicted by eq 3. The initial distribution of solvated electrons may be approximated by the exponential function

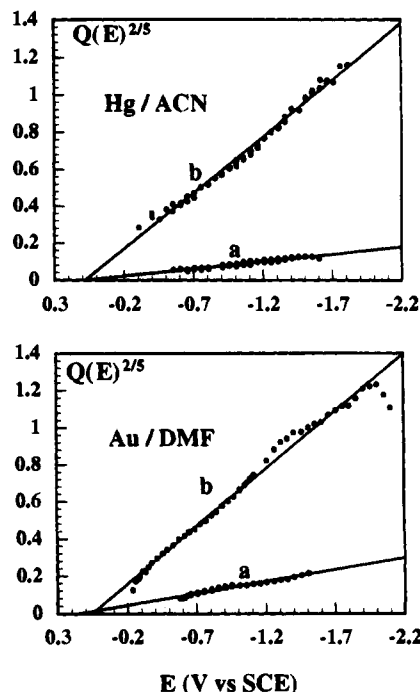


**Figure 4.** Test of the  $5/2$  power law in acetonitrile and DMF (+0.1 M  $\text{Et}_4\text{NClO}_4$ ) in the absence (a) and presence (b) of 4-bromoanisole (60 and 34 mM, respectively). The y-axis is normalized toward the value of  $Q(E)^{2/5}$  at  $-1.6$  V vs SCE in the presence of the scavenger.

**Table 1.** Values of the Threshold Potential in DMSO, DMF, and Acetonitrile (in V vs SCE)

	DMF <sup>a</sup>	DMSO <sup>b</sup>	acetonitrile <sup>b</sup>
4-bromoanisole	0.08	0.15	0.13
4-methylbenzyl chloride	0.06		0.09

<sup>a</sup> Au. <sup>b</sup> Hg.

defined in eq 7.

$$f(x) = \frac{\exp(-x/l_s)}{l_s} \quad (7)$$

Under these conditions, the function  $F(E, C^0)$  should depend upon scavenger concentration as shown in eq 8.

$$F(E, C^0) = \frac{l_s}{l_s + l_e} = \frac{l_s}{l_s + \left(\frac{D_e}{k_e C^0}\right)^{1/2}} \quad (8)$$

and therefore:

$$\frac{Q(E)}{Q_0} = [1 + n(E)] \frac{l_s}{l_s + \left(\frac{D_e}{k_e C^0}\right)^{1/2}} \quad (9)$$

It is indeed observed (Figure 7a) that, both at the foot ( $E = -1.00$ ,  $E = -1.15$  V vs SCE) and at the top ( $E = -1.40$ ,  $E = -1.50$  V vs SCE) of the polarogram, the relative value of the photoinjected charge,  $Q(E)/Q_0$ , begins to bend downward as the concentration increases as predicted from eq 9. The fact that eq 9 is quantitatively followed is shown in Figure 7b since, as indicated by eq 10 which derives immediately from eq 9,  $Q(E)/Q_0(C^0)^{1/2}[1 + n(E)]$  varies linearly with  $Q(E)/Q_0$ .

$$\frac{Q(E)}{Q_0 \sqrt{C^0} [1 + n(E)]} = l_s \left(\frac{k_e}{D_e}\right)^{1/2} \left[1 - \frac{1}{[1 + n(E)]} \frac{Q(E)}{Q_0}\right] \quad (10)$$

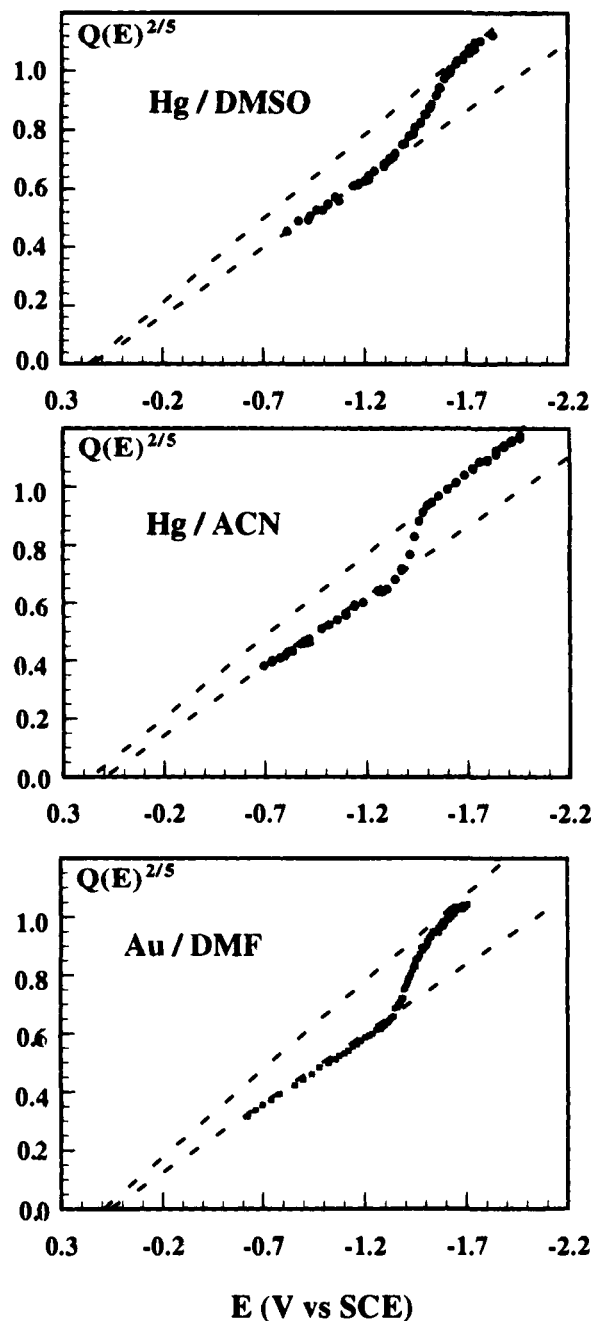


**Figure 5.** Test of the  $5/2$  power law for the DMSO, acetonitrile, and DMF (+0.1 M  $\text{Et}_4\text{NClO}_4$ ) in the presence of 4-methylbenzyl chloride (60 mM). The y-axis is normalized toward the value of  $Q(E)^{2/5}$  at  $-1.6$  V vs SCE.

That this prediction is indeed correct is shown in Figure 7b where it is observed that, at the foot and at the top of the benzyl radical polarogram, eq 10 is satisfactorily obeyed. The value of  $l_s(k_e/D_e)^{1/2}$  that can be derived from the linear plot in Figure 7b,  $0.75 \text{ M}^{-1/2}$ , corresponds to a value of  $l_s$ , the mean thickness of the solvated electron distribution, that is on the order of  $2.5\text{--}7.5 \text{ \AA}$  (taking for  $k_e$  the diffusion limit,  $\approx 10^{10} \text{ M}^{-1} \text{ s}^{-1}$ , and  $D_e = 10^{-5}\text{--}10^{-4} \text{ cm}^2 \text{ s}^{-1}$ ).

It is also interesting to estimate the total amount and the concentration of radicals formed under typical experimental conditions. The double layer capacitance is on the order of  $10 \mu\text{F cm}^{-2}$ . Since the photopotentials are comprised between 0.5 and 2 mV, the photoinjected charges fall in the range  $5 \times 10^{-9}\text{--}2 \times 10^{-8} \text{ C cm}^{-2}$  which corresponds to  $5 \times 10^{-14}\text{--}2 \times 10^{-13} \text{ mol of radicals per cm}^{-2}$  formed at the electrode surface. At a typical observation time,  $200 \mu\text{s}$ , the diffusion length of the

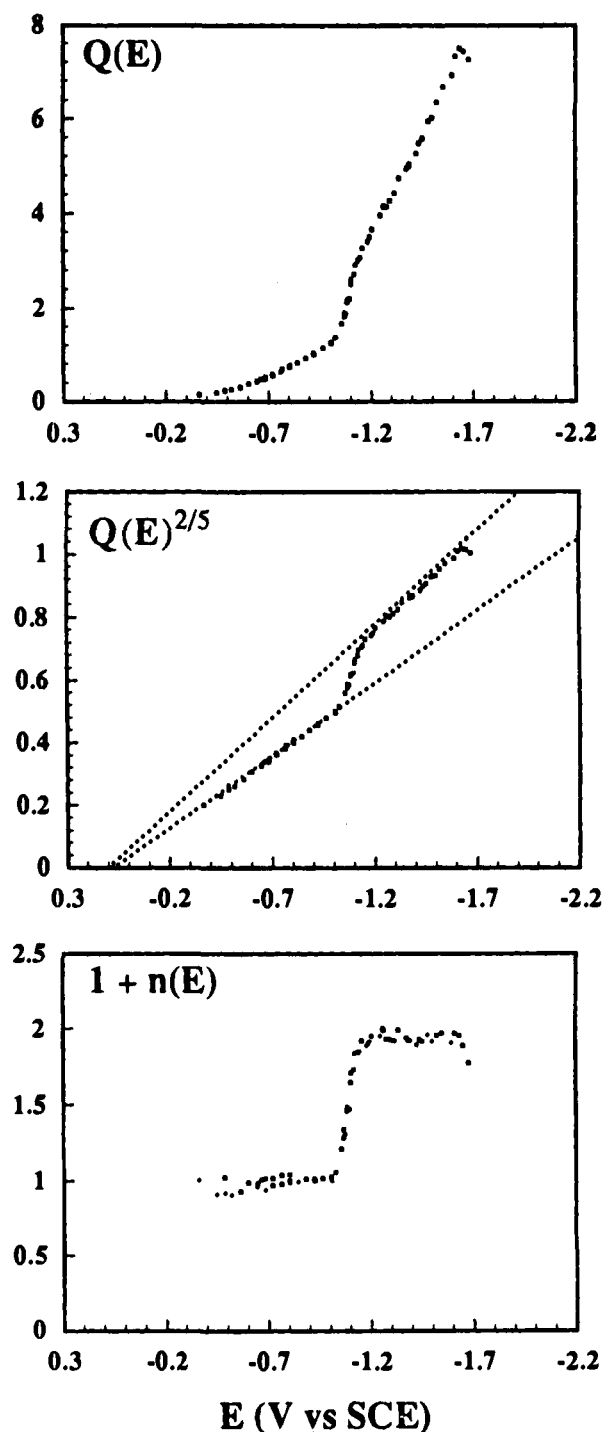


**Figure 6.** Extraction of the polarogram of diphenylmethyl radical from the raw data obtained with diphenylmethyl chloride (52 mM) in DMF (+0.1 M  $\text{Et}_4\text{NClO}_4$ ) at a gold electrode. The y-axes are normalized so as  $Q(E)^{2/5}$  at  $-1.6$  V vs SCE equals 1.

radicals,  $l_R = (D_R t)^{1/2} = 4.5 \times 10^{-5} \text{ cm}$ . The radical concentration thus ranges from  $10^{-6}$  to  $4 \times 10^{-6} \text{ M}$ .

Other examples of radical polarograms are shown in Figures 8 and 9. The various half-wave potentials that we have measured are summarized in Table 2.

We have observed that DMF is the most convenient of the three solvents in the sense that scavenging of the radical by the solvent is minimal. Small background photocurrents are then observed, and the radical polarograms can be recorded with smaller concentrations of the radical generating substrate.

We note that when the same radical is generated from different substrates, the half-wave potential is, as expected, the same in the same solvent and at the same electrode.

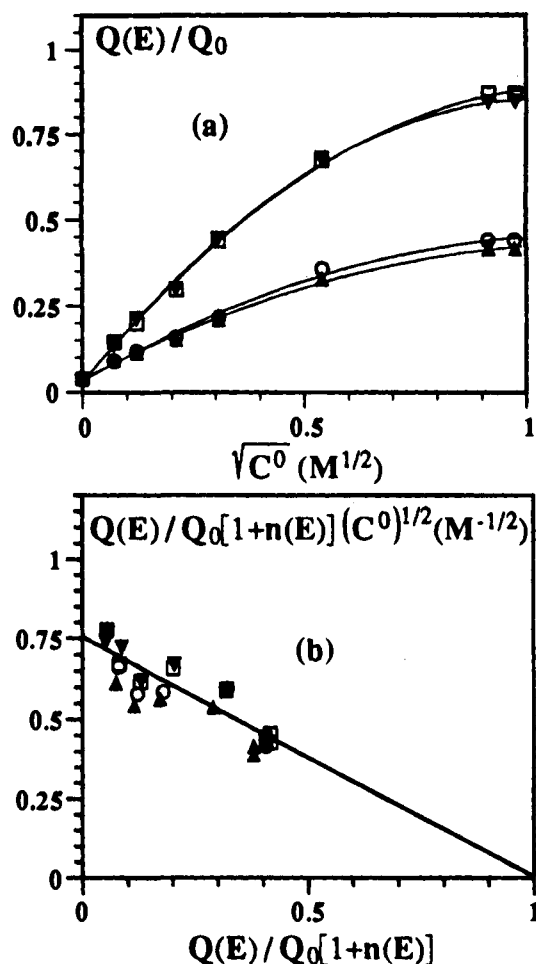


**Figure 7.** Photoinjection of electrons from a gold electrode into DMF (0.1 M  $Et_4ClO_4$ ) containing benzyl bromide: (a) variation of the photocharge with scavenger concentration and (b) testing of eq 10; dc potential:  $-1.00$  (▲),  $-1.15$  (○),  $-1.40$  (▼),  $-1.50$  (□) V vs SCE.

In the same solvent, the half-wave potentials do not differ much from a gold to a mercury electrode indicating that the interactions of the radicals and the electrode metal are weak. There is a systematic trend for the half-wave potentials to be slightly more negative on mercury than on gold which may be a reflection of different metal-radical interactions and/or of different influences the double layer on the electron transfer kinetics. With mercury, more difficulties were encountered with the substrates than with the radicals: meaningful results could be obtained with chlorides and cations but not with bromides in line with the increased tendency to form organomercury derivatives.

It is also observed that, at the same electrode, the value of the half-wave potentials do not vary much from one solvent to the other.

The literature data that can be compared the most easily with the present results are those that have been obtained by solution photogeneration of radicals,<sup>9,10</sup> although acetonitrile was exclusively used as solvent in these determinations. The pertinent data are listed in Table 2. We see that there is a general agreement between the two sets of data although the half-wave potentials from the present work tend to be slightly more positive than those from ref 9d. A likely reason for these differences is that the kinetics of the various reactions in which the radical and the resulting carbanion are engaged as well as those of the electron transfer itself may affect diversely the difference between the half-wave potential and the formal potential of the radical/carbanion couple in each method.

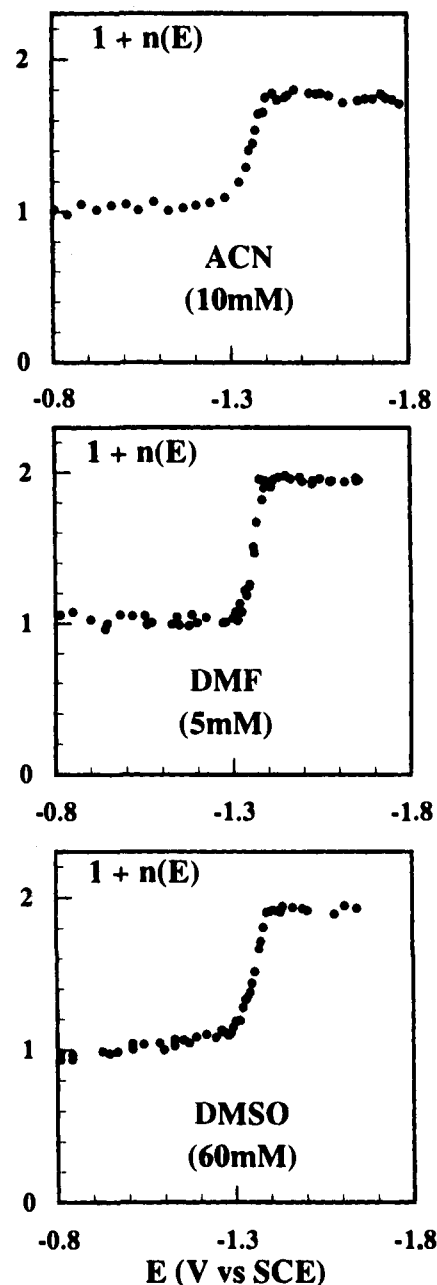


**Figure 8.** Polarograms of substituted benzyl radical in various solvent at a mercury electrode obtained from benzyl chloride (the concentration is indicated on each curve).

## Experimental Section

**Instrumentation and Procedures.** A three-electrode cell, placed in a Faraday cage, with a platinum counter electrode and an aqueous saturated calomel reference electrode (separated from the solution by a bridge filled with the solvent and the supporting electrolyte) was used throughout the work. The working electrode was either a 0.5 mm-diameter gold disk (polished with diamond paste, ultrasonically rinsed in ethanol and cleaned by cycling between  $-0.6$  and  $0.9$  V in an 1 M sulfuric acid aqueous solution before each run) or a mercury drop deposited on a 0.5 mm-diameter gold disk. The solution was degassed with argon before each run and maintained under an argon stream during each experiment.

A block-diagram of the pulsed laser photochemical setup is shown in Figure 2. The light source was a XeCl excimer laser (Questek 2054, wavelength/308 nm, pulse duration: 20–50 ns, pulse stability:  $\pm 5\%$ ). The laser beam was focused onto the electrode surface by means of a system of lenses, mirrors, and optical filters so as to obtain an intensity of 50 kW/cm<sup>2</sup> and to cover an area slightly larger than the electrode surface area. Quartz light-guides were used so as to keep constant the

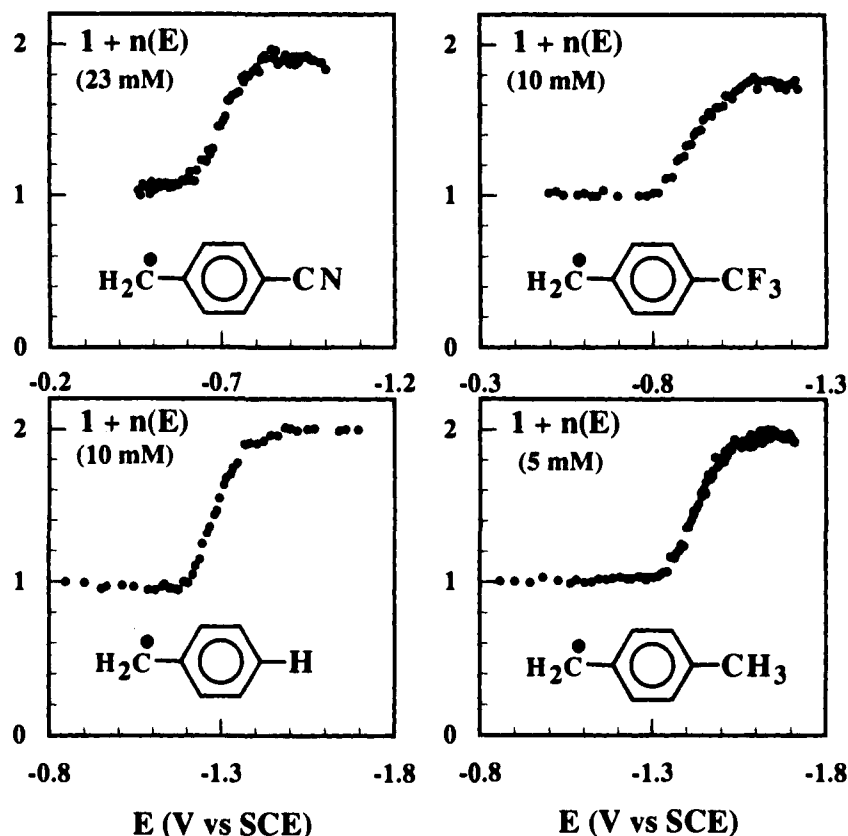


**Figure 9.** Polarograms of substituted benzyl and substituted benzyl radicals obtained from the parent bromides (the concentration is indicated on each curve) in DMF (+0.1 M  $\text{Et}_4\text{NClO}_4$ ) at a gold electrode.

**Table 2.** Radical Half-Wave Potentials (in V vs SCE)

radical	X	DMF		DMSO		acetonitrile	
		Hg	Au	Hg	Au	Hg	Au
$\text{Ph}_2\text{CH}^\bullet$	Cl	-1.12	-1.05	-1.07		-1.16	-1.14 (-1.14) <sup>a</sup>
$\text{PhCH}_2^\bullet$	Br		-1.08				
	Cl	-1.37	-1.34	-1.36	-1.32	-1.35	(-1.43) <sup>a</sup>
$\text{PhCH}_2^\bullet$	Br		-1.37				
	$\text{NMe}_3^+$	-1.36	-1.34				
3-MePhCH <sub>2</sub> <sup>•</sup>	Cl	-1.36	-1.31	-1.36			(-1.50) <sup>a</sup>
4-MePhCH <sub>2</sub> <sup>•</sup>	Cl	-1.43	-1.39	-1.43		-1.46	-1.43 (-1.60) <sup>a</sup>
	Br		-1.40				
4-Cl-PhCH <sub>2</sub> <sup>•</sup>	Cl <sup>-</sup>	-1.28	-1.2				(-1.40) <sup>a</sup>
3-CF <sub>3</sub> -PhCH <sub>2</sub> <sup>•</sup>	Cl <sup>-</sup>	-1.17	-1.04	-1.16		-1.20	-1.13
4-CF <sub>3</sub> -PhCH <sub>2</sub> <sup>•</sup>	Br <sup>-</sup>		-0.89				
3-CN-PhCH <sub>2</sub> <sup>•</sup>	Cl <sup>-</sup>	-1.14		-1.15			(-1.11) <sup>a</sup>
4-CN-PhCH <sub>2</sub> <sup>•</sup>	Cl <sup>-</sup>	-0.93	-0.69	-0.93		-0.905	-0.74 (-0.77) <sup>a</sup>
	Br <sup>-</sup>		-0.68				

<sup>a</sup> From ref 9d.

light path (1 mm) in the solution. The photopotentials were measured by means of a Nicolet 310 digital oscilloscope.

For each value of the dc potential,  $E$ , the measurement of the photopotential is repeated at least ten times. The signals are transferred and average in the computer (PC 386). Then a new value of  $E$  is set, and a new set of experiments is carried out. Under these conditions, the reproducibility of photopotentials was found to be better than 3%.

**Chemicals.** Solvents (DMF and DMSO, HPLC grade from Burdick & Jackson, acetonitrile Uvasol from Merck) were of the highest purity grade and used without further purification. As supporting electrolyte we used tetraethylammonium perchlorate (Fluka, Puriss). 4- and 3-Cyanobenzyl chlorides were prepared by refluxing the corresponding bromides with a tenfold excess of  $\text{Et}_4\text{NCl}$  in a methylene chloride-acetone mixture. All other substrates were commercially available (Aldrich).

## Conclusions

Laser pulse photoinjection of electrons allows the determina-

tion of radical reduction polarograms from generating substrates that are more difficult to reduce than the radical, thus complementing the direct electrochemical method. Reproducible values of half-wave potentials can thus be determined that agree reasonably well with previous literature when available. Further investigation of the influence of kinetic factors on the half-wave potentials by means of time-resolved experiments seems however in order to reach the corresponding formal potentials. Improvement of temporal resolution may also reveal interesting chemistry of the observed radicals.

**Acknowledgment.** We are indebted to Marc Robert (Laboratoire d'Electrochimie Moléculaire de l'Université Denis Diderot) for the gift of samples of 4- and 3-cyanobenzyl chlorides.

JA943356H